

**EXPERIMENTAL AND COMPUTATIONAL
FLUID DYNAMICS (CFD) ANALYSIS OF
WIND-INDUCED NOISE IN TWO-WAY RADIO**

UMMI MASYITAH BINTI MOHD FISOL

UNIVERSITI SAINS MALAYSIA

2016

EXPERIMENTAL AND COMPUTATIONAL FLUID DYNAMICS (CFD)
ANALYSIS OF WIND-INDUCED NOISE IN TWO-WAY RADIO

by

UMMI MASYITAH BINTI MOHD FISOL

Thesis submitted in fulfillment of the
requirements for the Degree of
Master of Science

September 2016

ACKNOWLEDGEMENT

“In the name of ALLAH, The Most Gracious and The Most Merciful”

I would like to express my deepest gratitude to my supervisors, Dr Norilmi Amilia Ismail and Prof. Dr. Zaidi Mohd Ripin, for their excellent guidance, caring and patience for guiding me through this research. I have gain an experience which I cannot get anywhere else and I truly appreciate the opportunity to work under their supervision.

My special thanks to the technicians of School of Mechanical and Aerospace Engineering for helping me to complete the experiment. They are Mr. Mahmud bin Isa, Mr Ridhwan, Mr Baharom Awang, Mr Wan Mohd Amri Wan Mamat Ali, and other technicians who I missed to mention their names.

I would like to thank my friends from The Vibration Laboratory, Dr Najib, Mr Zhafran, Chan Ping Yi, Vigren and Mohd Khairul Rabani for guiding my research. They helped me a lot in this research until the completion. Without them, I will not finish my work on time.

To those who indirectly contributed in this project, your gentleness means a lot to me. Thank you very much. Last but definitely not least, my deepest and most heart-felt gratitude to my husband, Ahmad Ashraf bin Mohamad for always be by my side, my parents, sisters and brothers. They are always supporting me and encouraging me with their best wishes.

TABLE OF CONTENTS

	Page
ACKNOWLEDGEMENT	ii
TABLE OF CONTENTS	iii
LIST OF TABLES	vi
LIST OF FIGURES	viii
LIST OF SYMBOLS	xii
LIST OF ABBREVIATIONS	xiii
ABSTRAK	xiv
ABSTRACT	xvi
CHAPTER ONE – INTRODUCTION	
1.1 Background	1
1.2 Problem Statement	2
1.3 Objectives of Research	3
1.4 Scope of Study	3
1.5 Thesis Outline	5
CHAPTER TWO - LITERATURE REVIEW	
2.1 Introduction	6
2.2 Wind-Induced Noise	6
2.2.1 Wind-Induced Noise in Microphones	6
2.2.2 Wind-Induced Noise in Aerodynamic and Mechanical Sources	8
2.3 Vortex Shedding Phenomenon	9
2.4 Wind-Induced Noise Simulation	15
2.5 Summary	18

CHAPTER THREE - METHODOLOGY

3.1	Introduction	19
3.2	Sound Measurement	19
3.2.1	Two-way Radio	19
3.2.2	Experimental of Cavity Specimen	23
3.3	Computational Fluid Dynamics (CFD)	28
3.3.1	Introduction	28
3.3.2	Geometry and Mesh	29
3.3.3	Simulation Setup	35
3.3.4	Solution and Results	37
3.3.5	Root-Mean-Square Error (RMSE)	39

CHAPTER FOUR - RESULT AND DISCUSSIONS

4.1	Introduction	40
4.2	Noise Measurement	40
4.2.1	Measurement of Two-Way Radio	40
4.2.1.1	WindVelocity	42
4.2.1.2	Angle of Attack	44
4.2.2	Experimental Results of Specimen Cavity	46
4.2.2.1	Experimental Result on Baseline Model Without Cavity	48
4.2.2.2	Experimental Results of Specimen with Cavity	50
4.2.2.3	Influence of Wind Velocity and Cavity Position	55
4.3	Computational Fluid Dynamics (CFD)	56
4.3.1	Model of 2D and 3D Cavity	56
4.3.1.1	CFD Simulation Result of 2D Geometry - Cavity Position	58

4.3.1.2	CFD Simulation Result of 2D Geometry - Wind Velocity	74
4.3.1.3	CFD Simulation Result of Cavity in 3D Geometry	89
4.3.2	Validation of CFD Model	92
4.3.2.1	Root-Mean-Square Error (RMSE)	96

CHAPTER FIVE - CONCLUSIONS

5.1	Conclusion	97
5.2	Recommendations for Future Works	99

REFERENCES	100
------------	-----

APPENDICES

Appendix A: Accelerometer

Appendix B: Model of Accelerometer

LIST OF PUBLICATIONS

LIST OF TABLES

		Page
Table 2.1	Types of sound sources	12
Table 3.1	Position of angle of attack for the two-way radio	23
Table 3.2	Reynolds Number calculation	25
Table 3.3	Geometry of rectangular cavities	29
Table 3.4	Discretization used in the simulation	37
Table 3.5	Under relaxation factors used in the simulation	37
Table 4.1	Highest peak SPL at P1	50
Table 4.2	Highest peak SPL at P2	51
Table 4.3	Highest peak SPL at P3	52
Table 4.4	Highest peak SPL at P4	54
Table 4.5	Highest peak of SPL at P5	55
Table 4.6	Summary of experimental result	55
Table 4.7	Velocity contour for wind velocity of 0.75 m/s at the cavity floor	59
Table 4.8	Velocity contour for wind velocity of 1.49 m/s at the cavity floor	63
Table 4.9	Velocity contour for wind velocity of 2.24 m/s at the cavity floor	66
Table 4.10	Velocity contour for wind velocity of 2.99 m/s at the cavity floor	69
Table 4.11	Velocity contour for wind velocity of 3.74 m/s at the cavity floor	72
Table 4.12	Velocity contour at the cavity floor at P1	76
Table 4.13	Velocity contour at the cavity floor at P2	78
Table 4.14	Velocity contour at the cavity floor at P3	81

Table 4.15	Velocity contour at the cavity floor at P4	85
Table 4.16	Velocity contour at the cavity floor at P5	87

LIST OF FIGURES

		Page
Figure 1.1	Vortex Shedding phenomenon induced by wind flowing over a cylinder	1
Figure 1.2	Basic Configuration of two-way radio	2
Figure 1.3	Cross section of two-way radio microphone cavity	4
Figure 2.1	Velocity field and vortex shedding (Jianu et al. (2012)).	10
Figure 2.2:	Oil-film visualization results for the wall-mounted finite airfoil with $L/T=16.7$ at U_∞ of (a) 35 m/s and (b) 25 m/s	11
Figure 2.3:	Three typical vortex shedding patterns of (a) Individual vortex shedding formed, (b) Twin vortex street symmetrically formed and (c) Large Karman vortex street	14
Figure 2.4:	Trash rack model with different angles	16
Figure 2.5	Vorticity contour of flow past the opening for different types of trash racks in the x-z mid-plane for (a)	17
Figure 3.1	Schematic diagram of wind tunnel testing	20
Figure 3.2	Experimental setup for wind tunnel testing with location of left-to-right and right-to-left wind flow direction	21
Figure 3.3	Wind direction and angle of attack of the experimental setup	23
Figure 3.4	Fabricated specimen with five holes of (a) full view of baseline model and (b) side view of specimen with cavities	24
Figure 3.5	Experimental setup of wind tunnel testing	27
Figure 3.6	Flow of CFD simulation	28
Figure 3.7	The two-dimensional geometry with selected medium mesh	31
Figure 3.8	The two-dimensional geometry with finer mesh	32
Figure 3.9	The two-dimensional geometry with coarser mesh	32
Figure 3.10	Three-dimensional geometry at P1	33

Figure 3.11	Meshing of three-dimensional geometry	33
Figure 3.12	Rectangular cavity drawn in CFD	34
Figure 3.13	Meshing of CFD simulation	35
Figure 3.14	General setup for FLUENT	36
Figure 3.15	Sample of rakes at P2 for rectangular cavities model	38
Figure 3.16	Sample of rakes for validation of CFD model	39
Figure 4.1	FFT from wind tunnel testing of two-way radio with (a) Wind tunnel structural acceleration, (b) Ambient noise and (c) Received wind noise	41
Figure 4.2	Graph of pressure against frequency of (a) left-to-right flow, (b) right-to-left flow with different wind velocities	44
Figure 4.3	Graph of pressure against frequency of (a) left-to-right flow and (b) right-to-left flow with different angles	45
Figure 4.4	FFT from wind tunnel testing of rectangular cavities at P5 of (a) Wind tunnel structural acceleration, (b) Ambient noise and (c) Received signal	47
Figure 4.5	Graph of SPL against frequency at wind velocity of 0.75 m/s for baseline (a) model and (b) specimen with cavity	49
Figure 4.6	Graph of SPL against frequency at P1 with cavities	50
Figure 4.7	Graph of SPL against frequency at P2 with cavities	51
Figure 4.8	Graph of SPL against frequency at P3 with cavities	52
Figure 4.9	Graph of SPL against frequency at P4 with cavities	53
Figure 4.10	Graph of SPL against frequency at P5 with cavities	54
Figure 4.11	Mesh Independence Study of (a) coarse mesh (b) selected medium mesh of 2D geometry at P5	57
Figure 4.12	Velocity contour at wind velocity of 0.75 m/s for (a) P1, (b) P2, (c) P3, (d) P4, and (e) P5	58
Figure 4.13	Velocity profile at wind velocity of 0.75 m/s	59
Figure 4.14	Vorticity contour at wind velocity of 0.75 m/s for (a) P1, (b) P2, (c) P3, (d) P4, and (e) P5	60

Figure 4.15	Velocity contour at wind velocity of 1.49 m/s for (a) P1, (b) P2, (c) P3, (d) P4, and (e) P5	62
Figure 4.16	Velocity profile at wind velocity of 1.49 m/s	62
Figure 4.17	Vorticity contour at wind velocity of 1.49 m/s for (a) P1, (b) P2, (c) P3, (d) P4, and (e) P5	63
Figure 4.18	Velocity contour at wind velocity of 2.24 m/s for (a) P1, (b) P2, (c) P3, (d) P4, and (e) P5	65
Figure 4.19	Velocity profile at wind velocity of 2.24 m/s	65
Figure 4.20	Vorticity contour at wind velocity of 2.24 m/s for (a) P1, (b) P2, (c) P3, (d) P4, and (e) P5	66
Figure 4.21	Velocity contour at wind velocity of 2.99 m/s for (a) P1, (b) P2, (c) P3, (d) P4, and (e) P5	68
Figure 4.22	Velocity profile at wind velocity of 2.99 m/s	68
Figure 4.23	Vorticity contour at wind velocity of 2.99 m/s for (a) P1, (b) P2, (c) P3, (d) P4 and (e) P5	69
Figure 4.24	Velocity contour at wind velocity of 3.74 m/s for (a) P1, (b) P2, (c) P3, (d) P4, and (e) P5	71
Figure 4.25	Velocity profile at wind velocity of 3.74 m/s	71
Figure 4.26	Vorticity contour at wind velocity of 3.74 m/s for (a) P1, (b) P2, (c) P3, (d) P4, and (e) P5	73
Figure 4.27	Velocity contour for cavity position at P1 of (a) 0.75 m/s, (b) 1.49 m/s, (c) 2.24 m/s, (d) 2.99 m/s and (e) 3.74 m/s	75
Figure 4.28	Velocity profile for cavity position at P1	75
Figure 4.29	Vorticity contour for cavity position at P1 of (a) 0.75 m/s, (b) 1.49 m/s, (c) 2.24 m/s, (d) 2.99 m/s and (e) 3.74 m/s	76
Figure 4.30	Velocity contour for cavity position at P2 of (a) 0.75 m/s, (b) 1.49 m/s, (c) 2.24 m/s, (d) 2.99 m/s and (e) 3.74 m/s	77
Figure 4.31	Velocity profile for cavity position at P2	78
Figure 4.32	Vorticity contour for cavity position at P2 of (a) 0.75 m/s, (b) 1.49 m/s, (c) 2.24 m/s, (d) 2.99 m/s and (e) 3.74 m/s	79
Figure 4.33	Velocity contour for cavity position at P3 of (a) 0.75 m/s, (b) 1.49 m/s, (c) 2.24 m/s, (d) 2.99 m/s and (e) 3.74 m/s	80

Figure 4.34	Velocity profile for cavity position at P3	81
Figure 4.35	Vorticity contour for cavity position at P3 of (a) 0.75 m/s, (b) 1.49 m/s, (c) 2.24 m/s, (d) 2.99 m/s and (e) 3.74 m/s	82
Figure 4.36	Velocity contour for cavity position at P4 of (a) 0.75 m/s, (b) 1.49 m/s, (c) 2.24 m/s, (d) 2.99 m/s and (e) 3.74 m/s	84
Figure 4.37	Velocity profile for cavity position at P4	84
Figure 4.38	Vorticity contour for cavity position at P4 of (a) 0.75 m/s, (b) 1.49 m/s, (c) 2.24 m/s, (d) 2.99 m/s and (e) 3.74 m/s	85
Figure 4.39	Velocity contour for cavity position at P5 with wind velocity of (a) 0.75 m/s, (b) 1.49 m/s, (c) 2.24 m/s, (d) 2.99 m/s and (e) 3.74 m/s	86
Figure 4.40	Velocity profile for cavity position at P5	87
Figure 4.41	Vorticity contour for cavity position at P5 of (a) 0.75 m/s, (b) 1.49 m/s, (c) 2.24 m/s, (d) 2.99 m/s and (e) 3.74 m/s	88
Figure 4.42	Velocity contour of 3D geometry at wind velocity of 3.74 m/s for (a) P1, (b) P2, (c) P3, (d) P4 and (e) P5	90
Figure 4.43	Velocity profile at wind velocity 3.74 m/s of (a) 3D geometry and (b) 2D geometry	90
Figure 4.44	Velocity contour of 3D geometry at P5 with wind velocity of (a) 0.75 m/s, (b) 1.49 m/s, (c) 2.24 m/s, (d) 2.99 m/s and (e) 3.74 m/s	91
Figure 4.45	Velocity profile for cavity position at P5 of (a) 3D geometry and (b) 2D geometry	91
Figure 4.46	Velocity profile for wind velocity (a) 12 m/s and (b) 15 m/s	93
Figure 4.47	Velocity contour for the wind velocity of 12 m/s: (a) CFD simulation and (b) experimental work of Koschatzky et al. (2011)	94
Figure 4.48	Velocity contour for the wind velocity of 15 m/s: (a) CFD simulation and (b) experimental work of Koschatzky et al. (2011)	96

LIST OF SYMBOLS

St	Strouhal Number
Re	Reynolds Number
L/T	Length-to-thickness ratio
U	Free stream velocity
C_L	Lift coefficient
C_D	Drag coefficient
α_A	Angle of attack
ρ	Density
μ	Dynamic viscosity
k	Turbulent kinetic energy
ε	Turbulent dissipation rate
V_{obs}	Observed value
V_{assign}	Modelled value
V_W	Velocity of two-way radio
V_{CFD}	Velocity of CFD simulation
L_W	Length of working fluid of two-way radio
L_{CFD}	Length of working fluid of CFD simulation
Re_W	Reynolds Number of the two-way radio
Re_{CFD}	Reynolds Number of CFD simulation

LIST OF ABBREVIATIONS

CFD	Computational Fluid Dynamics
FFT	Fast Fourier Transform
PIV	Particle Image Velocimetry
RMSE	Root-Mean-Square Error
SIMPLE	Semi-Implicit Method for Pressure-linked Equations
SPL	Sound Pressure Level
RMSD	Root Mean Square Deviation

ANALISIS EKSPERIMEN DAN PERKOMPUTERAN DINAMIK BENDALIR DISEBABKAN KEBISINGAN ANGIN TERARUH DALAM RADIO DUA HALA

ABSTRAK

Kajian ini menyiasat aliran angin dan pembentukan vorteks di dalam rongga-rongga untuk memahami hubungan mereka terhadap kewujudan kebisingan semasa komunikasi menggunakan radio dua hala. Pengukuran kebisingan yang disebabkan oleh aliran angin daripada radio dua hala dan model berskala besar (spesimen) telah dijalankan dalam terowong angin gelung terbuka dan analisis perkomputeran dinamik bendalir dilakukan. Kesan daripada arah aliran angin, kelajuan angin 2, 6 dan 10 m/s, nombor Reynolds masing-masing 8694, 26083 dan 43471, dan sudut tirus (0-45 darjah) telah dibentangkan dalam pengukuran kebisingan angin radio dua hala. Pengukuran aras tekanan bunyi di dalam rongga-rongga dengan lima kelajuan angin yang berbeza dan jarak dari sumber angin telah dijalankan ke atas spesimen. Perkomputeran Dinamik Bendalir telah digunakan untuk mensimulasikan aliran angin ke atas model untuk memerhatikan pembentukan vorteks di dalam rongga-rongga dengan berbeza kedudukan rongga dan juga kelajuan angin. Pengesahan telah dilakukan dengan membandingkan simulasi dengan eksperimen *Koschitzky et al. (2011)* menggunakan geometri rongga yang sama untuk kelajuan angin 12 dan 15 m/s. Hasil kajian menunjukkan bahawa halaju angin telah menyebabkan kebisingan angin meningkat untuk kedua-dua arah aliran angin dengan memberi kesan yang lebih kepada aliran arah angin dari kiri ke kanan. Aras tekanan bunyi juga meningkat dengan peningkatan halaju angin dan kedudukan yang lebih jauh dari sumber angin, semakin tinggi dialami oleh aras tekanan bunyi. Simulasi perkomputeran dinamik bendalir menunjukkan vorteks yang lebih kukuh telah terbentuk pada pinggir, dinding dan lantai rongga. Pembentukan vorteks telah meningkat di kedudukan

rongga yang lebih jauh dan pada halaju angin yang lebih tinggi. Keputusan simulasi bersetuju dengan penemuan eksperimen dengan Ralat Punca Min Kuasa Dua. Hasil dari kajian ini sangat penting kepada penambah baikan reka bentuk radio dua hala dalam mengurangkan bunyi bising semasa komunikasi.

EXPERIMENTAL AND COMPUTATIONAL FLUID DYNAMICS (CFD) ANALYSIS OF WIND-INDUCED NOISE IN TWO-WAY RADIO

ABSTRACT

This research investigated the wind flow and formation of vortex shedding inside cavities to understand the relationship of those to the occurrence of noise during communication using two-way radio device. Noise measurement due to wind flow of a two-way radio and its bigger scale model (specimen) was conducted inside an open-loop wind tunnel. A Computational Fluid Dynamics (CFD) analysis was also performed. The effect of wind flow direction, wind velocity of 2, 6 and 10 m/s, Reynolds Number of 8694, 26083 and 43471, respectively and angle of attack (0-45 degrees) were presented in wind noise measurement for a two-way radio. Measurement of Sound Pressure Level (SPL) inside cavities with five different wind velocities and distances from wind source has been conducted on the specimen. CFD was used to simulate wind flow over a model to observe the formation of vortex shedding inside cavities with different cavity positions and wind velocity. Validation has been done by comparing CFD simulation with experimental work of Koschatzky *et al.* (2011) using the same geometry of cavity for wind velocity of 12 and 15 m/s. The result shows that the wind velocity has increased the wind noise for both direction of wind flow with stronger effect for the left-to-right flow. The SPL is also increased with the increased of wind velocity and the further position from wind source, the stronger SPL has been encountered. The CFD simulation shows a stronger vortex shedding has been formed at the edge, wall and floor of the cavity. The vortex shedding formation is increased at further cavity position and higher wind velocity. CFD simulation agrees with the finding of the experimental work with Root-Mean-Square Error (RMSE). The result from this research is very significant

for the improvement of a two-way radio design in reducing noise during communication.

CHAPTER ONE

INTRODUCTION

1.1 Background

Noise can be defined as an undesirable sound or audio disturbance, which is generated by a vibrating surface or turbulent fluid flow (Rogers, 2006). Sound propagates in the form of longitudinal waves with series of compressions and rarefactions in the air. Wind-induced noise can be generated by wind flowing over an element or through gaps and cavities between elements causing a formation of vortex shedding. Figure 1.1 shows vortex shedding induced by a flow over a cylinder. The low-pressure zones (blue colours) are formed when the boundary layer is separated from the cylinder. Thus, a pair of vortices is appeared rotating in different directions (Giosan, 2013).

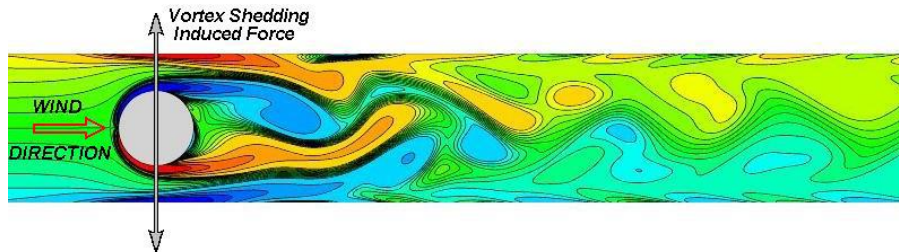


Figure 1.1: Vortex Shedding phenomenon induced by wind flowing over a cylinder

(Giosan, 2013)

Most of the studies discussed on wind-induced noise on the big building and microphone. The current study investigates the wind noise in two-way radio due to a circulation of flow in the cavity where the microphone is placed. A two-way radio is

a radio transceiver that used dedicated frequency for mobile communication. Figure 1.2 shows the general configuration of two-way radio.

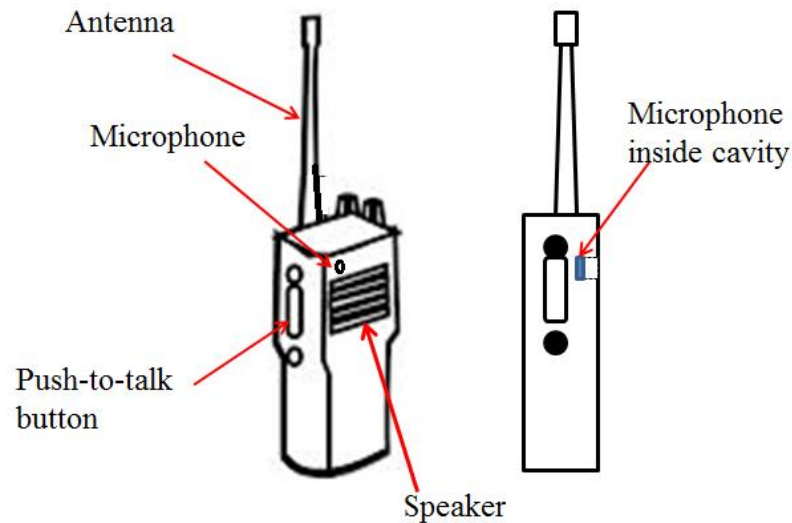


Figure 1.2: Basic Configuration of two-way radio

1.2 Problem Statement

Communication interference due to noise cannot totally be avoided in two-way radio during communication from the transmitter to the receiver. One of the criteria for a good two-way radio is to have less noise and higher speech quality. Most studies indicate the noise sources for two-way radio are from electrical and ambient noise. A various noise cancellation method based on these indications has been proposed. While talking, there is the wind coming from the mouth to the microphone of a two-way radio and this could be one of the sources of noise too. In addition, the level of noise increases in windy situations. These conditions are the reasons to study the relationship of wind flow to the occurrence of noise. Since the microphone is placed in a small hole in two-way radio, the possibility of flow trapped inside the cavity also needs to be investigated. It is expected that the

magnitude of the noise increases when the formation of vortices occurs inside the cavity of the microphone.

1.3 Objectives of Research

The objectives of this research are:

1. To analyse the pressure of the wind-induced noise over a two-way radio using experimental setup.
2. To analyse and determine the relationship of wind flow and cavity to the occurrence of wind-induced noise on a two-dimensional model of two-way radio microphone cavity using Computational Fluid Dynamics (CFD).

1.4 Scope of Study

Figure 1.3 shows a cross section of two-way radio microphone cavity. Figure 1.3 involves three fields of an engineering problem. The first field is the formation of vortex shedding from the air flow through the cavity, which is the fluid dynamics. The second field is the vibration of air inside the cavity after the air flow enters the cavity and hits the diaphragm. The last field is the acoustic when the air flow is transmitted to the wind noise by a microphone. Therefore, this research is focussed to the fluid dynamics and acoustic field where the formation of vortex shedding and effect of the wind-induced noise are investigated.

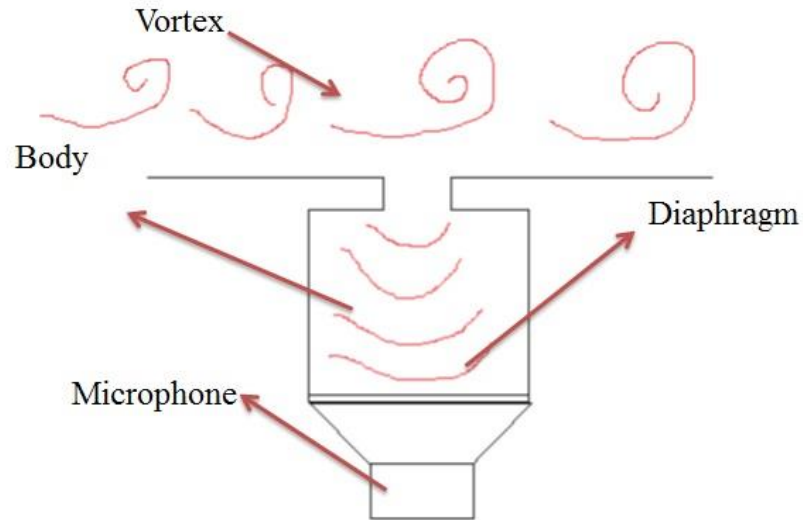


Figure 1.3: Cross section of two-way radio microphone cavity

The study covers noise measurement in an open-loop wind tunnel for two-way radio and a block with cavities made from Perspex to understand the fundamental of wind-induced occurrence. The measurement varies the wind velocity, the distance of the cavity from the wind source and also the angle of attack of the two-way radio. Computational Fluid Dynamics (CFD) is used to simulate the air flow over the two-dimensional and three-dimensional geometry of cavity where the formation of vortex shedding is studied. The wind source for both experiment and simulation was analysed with Reynolds Number of 8694, 17389, 26083, 34777 and 43471. CFD simulation of a single cavity is validated with the experimental work.

1.5 Thesis Outline

Chapter one presents the introduction, problem statement, research objectives and scope of the study.

Chapter two presents a critical review of literature of wind-induced noise, vortex shedding phenomenon, and wind-induced noise simulation.

Chapter three covers the methodology in this project. It includes a method to measure sound over a two-way radio, steps to fabricate a block with rectangular cavities, a CFD simulation on two-dimensional model of a block with rectangular cavities, validation of the CFD model, and the calculation of Root-Mean-Square Error (RMSE).

Chapter four presents the results and discussion of experimental and simulation work. It includes discussions on the relationship between wind velocity and cavity location to the strength of wind-induced noise, as demonstrated by results from experimental and simulation work.

Chapter five concludes this MSc research and suggests potential future work.

CHAPTER TWO

LITERATURE REVIEW

2.1 Introduction

Wind is one of the sources that contributed to the occurrence of noise. Nelke *et al.* (2012) stated that wind noise mainly occurs at low frequencies, so it is almost noise free in a large frequency range of speech. Wind noise occurs in the range of 0–500 Hz, with the main distribution at low frequencies and rapidly descending to high frequencies. This chapter reviews literatures related to wind-induced noise in microphones, aerodynamic and mechanical, vortex shedding phenomenon and wind-induced noise simulation.

2.2 Wind-Induced Noise

2.2.1 Wind-Induced Noise in Microphones

Wind noise is noise induced by wind and becomes significant when acoustical measurement is strongly affected by the wind (Nakasako *et al.* 2005). A strong correlation between wind noise and wind speed is well known to exist. The study carried out in wind induce noise were mostly on the noise of microphone. Ecotiere (2012) investigated the Sound pressure level (SPL) that can be affected by wind-induced noise at a screened microphone. SPL is used to measure noise level. The contribution of wind noise, which results in the SPL measurement, depends on the source noise level and wind characteristics, such as wind speed and atmospheric stability. The SPL of wind noise was estimated by Nakasako *et al.* (2005) in the form